Correlator Implementation for Orthogonal CSS Used in an Ultrasonic LPS

M. Carmen Peréz Rubio, *Member, IEEE*, Rebeca Sanz Serrano, Jesús Ureña Ureña, *Member, IEEE*, Álvaro Hernández Alonso, *Member, IEEE*, Carlos De Marziani, and Fernando J. Álvarez Franco, *Member, IEEE*

***Abstract*— This paper presents a new architecture for the correlation of orthogonal complementary sets of sequences (OCSS) and their performance in an ultrasonic local positioning system (U-LPS). OCSS are sets of sequences whose addition of correlation functions has ideal properties, that makes interference-free code-division multiple access (CDMA) possible. They can be used to encode the signals emitted by a CDMA-based U-LPS, enhancing the performance of such systems in terms of immunity against noise, multipath propagation, and near-far effect. Also, the orthogonality of the codes offers an operation resistance to multiaccess interference, which endows the U-LPS with the capability of simultaneous emission from different beacons. On the other hand, the detection of OCSS codes can be performed by means of efficient algorithms. This paper presents an optimization of previous proposals allowing the simultaneous correlation of OCSS by using fewer operations and memory elements. Furthermore, the hardware implementation of the proposed optimization is also addressed, and an U-LPS based on this proposal is presented.**

***Index Terms*— Code-division multiplexing, complementary sets of sequences, efficient correlation, ultrasonic local positioning system (U-LPS).**

I. Introduction

ORTHOGONAL complementary sets of sequences (OCSS) can improve the performance of code-division multiple access (CDMA) systems due to their correlation properties. Instead of unitary codes, OCSS works on a one-set of sequences-per-emitter basis, achieving perfect correlation properties when the sum of correlation functions of the corresponding sequences of each set is performed. Consequently, they can be used to mitigate the interferences in applications where multiple access, aperiodic emissions, asynchronous detection, near-far and multipath effects are common, as usual in local positioning systems based on pulse compression [1]– [5]. The use of this encoding technique can be also suitable for many other CDMA applications, such as mobile and wireless communications [6], non-destructive evaluation [7], spread spectrum time domain reflectometry [8], radar [9], optical fiber [11] and all applications that use OCSS as a kernel to construct zero correlation zone (ZCZ) codes [10] or inter-group complementary (IGC) codes [12]. Another important characteristic feature of OCSS is that they can be generated and correlated by means of efficient algorithms that reduce the computation requirements, when compared to straightforward methods [13], [14]. These algorithms can be further improved, thus making possible the real-time processing of the ultrasonic signals emitted by an Ultrasonic Local Positioning System (U-LPS), even when long OCSS are used.

In local positioning systems, the use of ultrasonic signals offers a low-cost solution with a centimetric precision at close ranges. CDMA techniques have been used to achieve multi-user access, robustness to noise and precision in distance measurements. Many of these systems [3]– [5] use traditional CDMA codes, such as Kasami or Gold, which are interference-limited. In consequence, they have to heavily rely on complex auxiliary systems to suppress the effects of both the inter-symbol interference (ISI) and multiple-access interference (MAI). That explains the considerable growth of the research devoted to improve the code design process in ultrasonic sensory systems. Examples using OCSS, or ZCZ codes constructed from OCSS, are [1], [14]– [16].

The correlation technique used to detect the codes determines the real-time operation capability of the system and limits the use of long codes. Hence, a lot of efforts are focused on the development of efficient correlator algorithms that reduce the computational load of the processing to achieve a hardware implementation capable to operate in real-time. First correlation algorithms, associated with complementary sets of two sequences, appear two decades ago [17]. Later, they have been extended to complementary sets of any number of sequences [18] and implemented in configurable hardware [19]. However, these approaches reduce the number of operations at the expense of a significant increase in memory requirements. More recently, an architecture is provided in [14] to directly obtain the sum of auto-correlation functions of the sequences belonging to a set, thus reducing the number of operations without penalizing memory requirements. Regard-

Manuscript received February 2, 2012; revised May 23, 2012; accepted May 31, 2012. Date of publication June 8, 2012; date of current version July 24, 2012. This work was supported in part by the Spanish Ministerio de Ciencia e Innovación under the LEMUR Project TIN2009-141 14-C04-01/04. The associate editor coordinating the review of this paper and approving it for publication was Prof. Ralph Etienne-Cummings.

M. C. P. Rubio, R. S. Serrano, J. U. Ureña, and Á. H. Alonso are with the Department of Electronics, University of Alcalá, Madrid 28805, Spain (e-mail: carmen@depeca.uah.es; rebeca.sanz@depeca.uah.es; urena@depeca.uah.es; alvaro@depeca.uah.es).

C. De Marziani is with the CONICET and Department of Electronics Engineering, National University of Patagonia San Juan Bosco, Comodoro Rivadavia 9000, Argentina (e-mail: marziani@unpata.edu.ar).

F. J. Á. Franco is with the Department of Electrical Engineering, Electronics and Automatics, University of Extremadura, Badajoz 06006, Spain (e-mail: fafranco@unex.es).

Color versions of one or more of the figures in this paper are available online at http://ieeexplore.ieee.org.

Digital Object Identifier 10.1109/JSEN.2012.2204046

ing OCSS, in [20] the simultaneous correlation of orthogonal complementary sets of two sequences by using a single correlation architecture is proposed. This architecture is extended in [21] to allow the simultaneous detection of M OCSS.

In this paper, OCSS are used to encode the emissions of several beacons located at known positions in the environment. Each beacon has assigned a different complementary set, orthogonal with those emitted by the other beacons. The beacons emit simultaneously and periodically their corresponding sets. Then, a non-limited number of mobile devices computes their positions asynchronously by hyperbolic trilateration of the distances obtained from the measurement of the Differences in Times Of Arrival (DTOA) among a reference beacon and the others. Hyperbolic trilateration avoids the use of additional hardware, such as radiofrequency or infrared signals, to synchronize emitters and receivers. To detect the DTOA, each mobile device performs the simultaneous correlation of the received signal with the sets assigned to each beacon and then subtracts the time delay corresponding to the reference beacon. To perform these correlations, the proposal in [21] is simplified to decrease operations and memory elements required in the correlation. This work also deals with the hardware design of the proposed optimization. It is based on configurable hardware (in Field Programmable Gate Arrays -FPGAs-) to gain the required flexibility in terms of correlator parameters. Thus, the user can change the configuration of the design according to the requirements of the U-LPS.

The rest of the paper is organized as follows: Section II introduces the correlation of OCSS. Section III provides a new architecture for the simultaneous correlation of OCSS. In Section IV the implementation in configurable hardware of such architecture is described. Then, Section V explains the U-LPS in which the proposed correlator is used, and Section VI shows some experimental results. Finally, the main conclusions of this work are outlined in Section VII.

II. Correlation of OCSS

Complementary sets of sequences achieve their ideal properties when the sum of auto-correlation functions (SACF) and the sum of cross-correlation functions (SCCF) of the sequences from each set is performed (1):

$$SACF = \sum_{j=0}^{M-1} C_{s_{i,j},s_{i,j}}[\tau] = M \cdot L \cdot \delta[\tau]$$
$$SCCF = \sum_{j=0}^{M-1} C_{s_{i,j},s_{i',j}}[\tau] = 0, \qquad i \neq i', \qquad \forall \tau \qquad (1)$$

where $C_{x,y}$ is the aperiodic correlation between x and y; $\{S_i; 0 \leq i \leq M-1\}$ are M mutually orthogonal sets, each one with M sequences $s_{i,j}$ of length L ($\{s_{i,j}[l]; 0 \leq j \leq M-1; 0 \leq l \leq L-1\}$) and elements $\in \{+1, -1\}$. That is, $s_{i,j}$ is the j-th sequence of the i-th set S_i. Note that number M of sequences in each set is equal to the number M of available orthogonal sets.

As mentioned before, the 4 beacons of the proposed U-LPS are encoded with 4 OCSS, each one with 4 sequences. Consider a more general case with M beacons. Then, M OCSS $\{S_i; 0 \leq i \leq M-1\}$, each one with M sequences $s_{i,j}$ of length L ($\{s_{i,j}[l]; 0 \leq j \leq M-1; 0 \leq l \leq L-1\}$) will be required. To transmit the M sequences $s_{i,j}$ assigned to a certain beacon, an M-ary modulation scheme (M-Phase Shift Keying, Frequency Shift Keying, etc.) or a time multiplexing modulation scheme (concatenation, interleaving, etc.) combined with a BPSK modulation can be used.

At the reception stage, after the demodulation, M correlators are required to detect the M sequences $s_{i,j}$ of a single set, and then to compute the sum of all these correlations. Since M orthogonal sets are transmitted to avoid interference among beacon emissions, M^2 correlators will be necessary. If the correlation of the OCSS is computed by means of conventional straightforward correlators, which require high computational cost, the system throughput is constrained. To reduce computations, methods based on Efficient Set of Sequences correlators (ESSC) [18] can be used. However, these approaches require more memory than the straightforward solution. Recently, in [14] it is proposed a new algorithm, called Transposed Efficient Set of Sequences Correlator (ESSC^T), that directly computes the sum of auto-correlation functions (SACF) without penalizing the memory requirements. This ESSC^T architecture has to be replicated M times to allow the detection of the M OCSS. Thus, each ESSC^T is matched to the emission from one of the beacons. This ESSC^T has been further improved in [21] to reduce the hardware requirements when M simultaneous OCSS have to be detected. It takes advantage of the orthogonality of the complementary sets and of the regular architecture of the ESSC^T to share the first $N-1$ stages for all the complementary sets and replicate $M-1$ times the last one for every orthogonal set. The number $N \in \mathbb{Z}^+$ of stages in the generator and correlator filters determines the final length $L = M^N$ of every sequence $s_{i,j}$. In this work, the common operations in the last stage are identified and, instead of being replicated $M-1$ times, it is simplified into one extra stage. Additionally, the architecture is modified into a regular and modular one that offers a more efficient hardware implementation. For a better understanding, Fig. 1 summarizes the tasks carried out in [14], in [21] and in the architecture proposed in this paper for the detection of M OCSS. Note that, in all figures, the SACF only appears in the output matched with the received set S_i.

III. Optimized Correlator for OCSS

This paper optimizes the previous contributions for a more efficient hardware implementation in two ways.

1) In [14] and [21] the internal links at every stage of the correlator, and the order of the inputs for each stage differ depending on the number M of sequences in the set, what makes difficult a generic hardware implementation. In this work the inputs at every stage are reorganized to obtain a regular and modular architecture that can be easily adapted to different values of M, thus allowing a more efficient hardware implementation.
2) The common operations in the correlation of the M OCSS are shared to minimize the computations to be carried out in their detection.

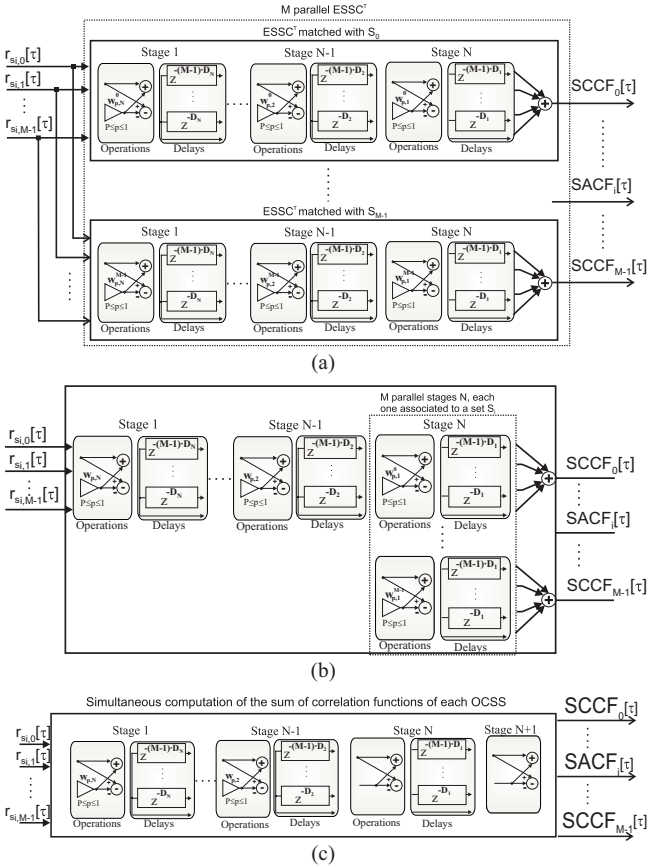

Fig. 1. Architectures for the detection of M OCSS. (a) M-times replication of the ESSC^T proposed in [14]. (b) M-times replication of the last stage (N) of the ESSC^T [21]. (c) Proposed correlator.

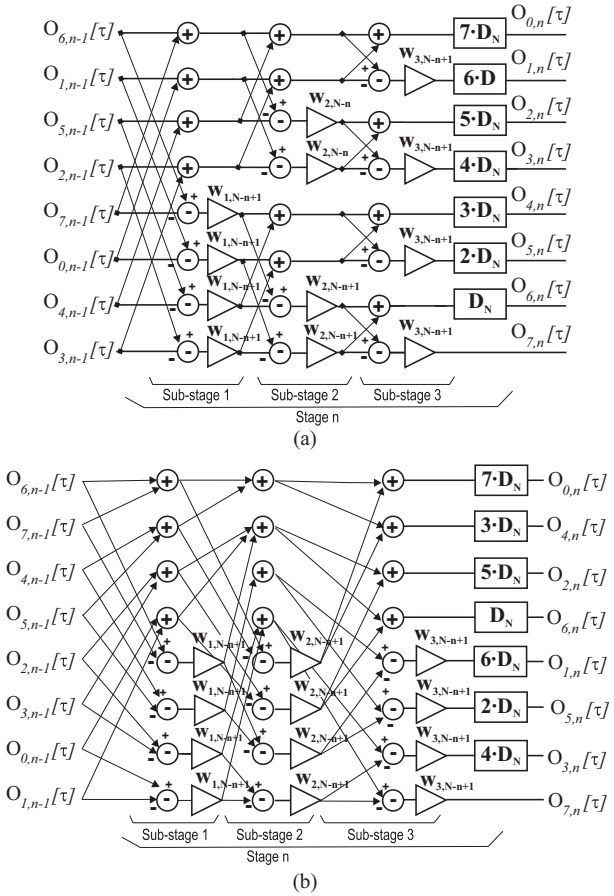

Fig. 2. (a) Stage n of the ESSC^T. (b) Stage n of the proposed correlator.

A. Transformation Into a Regular Structure

In a previous work [19], the similarities between the structure of the ESSC and the decimation-in-time Fast Fourier Transform (FFT) flow graph were exploited to make the ESSC architecture regular. By transposing the decimation-in-time FFT flow graph, a decimation-in-frequency algorithm is obtained whose architecture is similar to that from the ESSC^T. Thus, the variety of rearrangements of the FFT decimation-in-frequency algorithm can be applied to the ESSC^T. One of these rearrangements yields to a flow graph with the same geometry for each stage, what allows sequential data accessing and storage [25]. If the same technique is used to rearrange the links in the ESSC^T, a regular distribution for every stage can be obtained and the order of the inputs and outputs can be easily achieved for any value of M.

The transformation consists of rearranging the coefficients $d = \{M-1, M-2, \ldots, 1, 0\}$ that multiply the delays D_n at the output of each stage. With this purpose, the binary digits representing those d coefficients have to be sorted in bit-reversed order: starting with the least-significant bit instead of the most-significant bit as in ordinary sorting. As an illustration of this transformation, an example of a stage for the detection of a $M = 8$ complementary set is shown in Fig. 2. It can be observed that the delay $3 \cdot D_n$ ("011") for the proposed correlator in Fig. 2.(b) appears at the location previously occupied by the delay $6 \cdot D_n$ ("110") in the ESSC^T in Fig 2.(a). It can be observed that, after the rearrangement, a constant geometry is obtained which has the same interconnect pattern from sub-stage to sub-stage, independently on the number M of sequences in the set. Furthermore, the order of the input and output sequences at each stage can be easily obtained, in contrast with the complex recursive method that has to be used to obtain the input ordering in the previous proposals [18].

The connection between the position x of an input branch in a stage n and the sequence $O_{j,n-1}$ coming from the previous stage $n-1$ can be defined as follows:

$$\begin{aligned} &\text{For the even } x \text{ branches: } O_{M-2-x,n-1}[\tau] \\ &\text{For the odd } x \text{ branches: } O_{M-x,n-1}[\tau] \end{aligned} \tag{2}$$

where $x = 0$ is the input branch at the top of the flow graph and $x = M-1$ the input branch at the bottom; $O_{j,n}$ are the outputs obtained at stage n. Note that in the first stage ($n = 1$) of the algorithm, the inputs $O_{j,0}$ have to be connected to the received sequences $s'_{i,j}$ of the set S_i to be detected, that is, $O_{j,0} = s'_{i,j}$ ($s'_{i,j}$ are the sequences $s_{i,j}$ after received).

In the same way, if $0 \leq d \leq M-1$ represents the coefficients that multiply the delays D_n in a stage n, the sequence $O_{j,n}$ to be obtained at the output of every delay block $d \cdot D_n$ is $O_{M-1-d,n}[\tau]$.

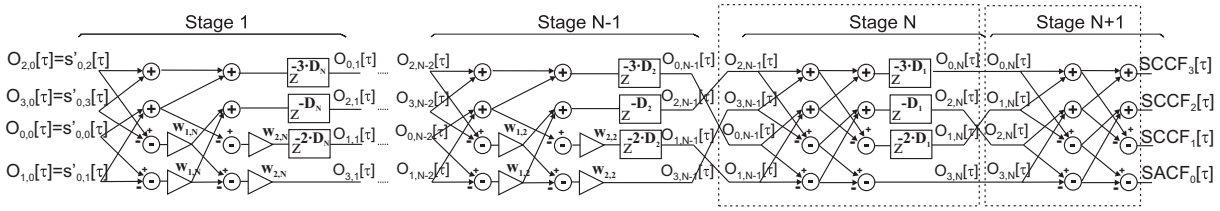

Fig. 3. Block diagram for the detection of $M = 4$ OCSS with length $L = 4^N$ in the proposed correlator.

B. Optimization in the Correlation of M OCSS

In the detection process, each orthogonal complementary set is different from the others in the last correlation stage $n = N$ thanks to the coefficients $\{w_{1,1}, w_{2,1}, \ldots, w_{P,1}\} \in \{+1, -1\}$; $P = log_2(M)$ [18]. Each combination of these coefficients provides the correlation with a different OCSS. This $n = N$ last stage can be replicated M times, and each replica be assigned a different combination of the $\{w_{1,1}, w_{2,1}, \ldots, w_{P,1}\}$ coefficients to obtain the simultaneous correlation with the M OCSS. This architecture is depicted in Fig. 1.(b). Note that in the figure, the superscript i, that indicates the complementary set S_i to be detected, only appears in the coefficients $w_{p,1}; 1 \leq p \leq P$ of stage N. The coefficients of the previous $0 \leq n \leq N-1$ stages are the same for all the M OCSS. There are operations between the M replicas of stage N that can be simplified to obtain a further optimization in the hardware required for the detection process.

Let $O^i_{j,N}$ denote the outputs at stage N associated to a complementary set S_i, where $i = \sum_{m=1}^{P} w_{m,1} \cdot 2^{m-1}$; $0 \leq i \leq M-1$ is the decimal representation of the coefficients $\{w_{1,1}, w_{1,2}, \ldots, w_{P,1}\}$ corresponding to this set S_i. Then, the case $O^{M-1}_{j,N}$ can be taken as a reference. For this particular case, the coefficients $\{w^{M-1}_{1,1}, w^{M-1}_{2,1}, \ldots, w^{M-1}_{P,1}\} = \{1, 1, \ldots, 1\}$ and can be omitted in the configuration of the last stage. A change in the coefficients $w^i_{p,1}$ to obtain the sum of correlations with other OCSS $S_i, i \neq M-1$ implies to invert the sign of some $\{O^{M-1}_{j,N}; 0 \leq j \leq M-1\}$ outputs according to the coefficients of a Hadamard matrix $\mathbf{H}$ of order M. That is, the elements $h_{M-i-1,j}; 0 \leq j \leq M-1$ in the column h_{M-i-1} of the Hadamard matrix $\mathbf{H}$ determines if the outputs $O^i_{j,N}$ have to be negated or not according to (3)

$$O^i_{j,N} = h_{M-i-1,j} \cdot O^{M-1}_{j,N}; \quad 0 \leq i, j \leq M-1. \tag{3}$$

For a better understanding, consider the case in (4) when $M = 4$.

$$\mathbf{H} = \begin{pmatrix} 1 & 1 & 1 & 1 \\ 1 & -1 & 1 & -1 \\ 1 & 1 & -1 & -1 \\ 1 & -1 & -1 & 1 \end{pmatrix}$$

i	$w_{2,1}$	$w_{1,1}$	$j=0$	$j=1$	$j=2$	$j=3$
0	0	0	$O^3_{0,N}$	$-O^3_{1,N}$	$-O^3_{2,N}$	$O^3_{3,N}$
1	0	1	$O^3_{0,N}$	$O^3_{1,N}$	$-O^3_{2,N}$	$-O^3_{3,N}$
2	1	0	$O^3_{0,N}$	$-O^3_{1,N}$	$O^3_{2,N}$	$-O^3_{3,N}$
3	1	1	$O^3_{0,N}$	$O^3_{1,N}$	$O^3_{2,N}$	$O^3_{3,N}$

(4)

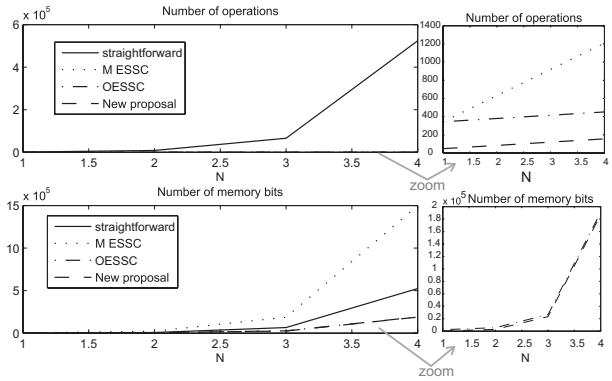

Fig. 4. Examples of the number of operations and memory resources required by correlators straightforward, ESSC^T, optimized ESSC^T (OESSC) and proposed correlator, when $M = 8$ OCSS are emitted simultaneously and the data-width at the input is $DW = 8$.

Thus, a more efficient architecture can be obtained for the correlation of M OCSS by modifying the architecture of Fig. 1.(b) as follows:

1) The multipliers $\{w_{1,1}, w_{2,1}, \ldots, w_{P,1}\}$ of stage N are eliminated.
2) The $M-1$ replicas of stage N are eliminated.
3) A combinational stage $N+1$ is included after the stage N to perform the additions and subtractions required to obtain the sum of correlations with all the M OCSS. Note that this additional stage include neither multipliers nor delay elements.
4) The j-th input branch of stage $N+1$ has to be connected to the output $O_{j,N}$ coming from the previous stage.
5) The sum of correlation functions with set S_i is obtained at the output branch $M-1-i$ of stage $N+1$. Remember that the branch 0 in any stage is the one at the top of the flow graph.

Fig 1.(c) summarizes the proposed transformation and Fig. 3 is an example when the received set is S_0 and $M = 4$. The SACF will be obtained at the output that matches with the received set S_i, the other outputs correspond to the SCCF with that set.

C. Efficiency of the New Architecture

A performance comparison between the proposed architecture, a straightforward implementation and the structures described in [14] and [21] has been achieved. Table I shows the calculations required to simultaneously detect M OCSS. Since only binary values are employed in the complementary

TABLE I
NUMBER OF OPERATIONS FOR THE SIMULTANEOUS CORRELATION OF M OCSS WITH DIFFERENT METHODS, AS A FUNCTION OF THE NUMBER M OF OCSS AND THEIR LENGTH $L = M^N$

Architecture	Adders	Products
Straightforward	$M^{(N+2)} - M$	$M^{(N+2)}$
M times replication of the ESSC^T [14]	$M^2 \cdot N \cdot log_2(M) + M^2 - M$	$\frac{N \cdot M^2}{2} \cdot log_2(M)$
Optimized ESSC^T [21]	$(M^2 + M \cdot N - M) \cdot log_2(M) + M^2 - M$	$\frac{M}{2} \cdot (M + N - 1) \cdot log_2(M)$
Proposed correlator	$(M \cdot N + M) \cdot log_2(M)$	$\frac{M}{2} \cdot (N - 1) \cdot log_2(M)$

TABLE II
MEMORY REQUIREMENTS FOR THE SIMULTANEOUS CORRELATION OF OCSS WITH DIFFERENT METHODS, AS A FUNCTION OF THE NUMBER M OF OCSS, THE CODE-LENGTH $L = M^N$ AND THE DATA-WIDTH DW AT THE INPUT

Architecture	Memory Positions
Straightforward	$DW \cdot M^{(N+1)} + M^{N+2}$
M times replication of the ESSC^T [14]	$\frac{M^3 - M^2}{2} \cdot \left(\frac{M^N - 1}{M-1} \cdot DW + \log_2(M) \cdot \sum_{i=1}^{N} i \cdot M^{N-i} \right)$
Optimized ESSC^T [21]	$\frac{M^2 - M}{2} \cdot \left(\frac{M^N + M^2 - 2M}{M-1} \cdot DW + log_2(M) \cdot (M \cdot N + \sum_{i=1}^{N-1} i \cdot M^{N-i}) \right)$
Proposed correlator	$\frac{M^2 - M}{2} \cdot \left(\frac{M^N - 1}{M-1} \cdot DW + log_2(M) \cdot \sum_{i=1}^{N} i \cdot M^{N-i} \right)$

sequences, the four implementations can be performed without any multiplication. However, multiplications have been included in the table to consider a general case where multilevel or polyphase values could be involved. Table II indicates the memory requirements for all the implementations.

For an easy comparison, Table III shows some examples of the computational load and memory bits required for the correlation of a received signal with M OCSS, when the A/D converter at the input is of $DW = 8$ bits. As can be seen, there is a remarkable improvement when the proposed correlator is used. Observe, for instance, the case $M = 16, L = 16$, where the number of stages is $N = 1$. In that case, the proposals in [14] and [21] offer the same results: they decrease the number of operations performed in comparison with a straightforward correlator, however they require more memory. On the contrary, the proposed correlator is the one that reduces more the number of computations involved, and also requires less memory than the straightforward implementation. When the number N of stages increases, the amount of saved resources is more significant, as can be observed in Fig. 4. It depicts the computational requirements for the correlation of $M = 8$ OCSS with different lengths $L = 8^N$.

IV. HARDWARE IMPLEMENTATION OF THE PROPOSED CORRELATOR

A parametric design with the correlator parameters specified in hardware synthesis has been developed. Then, the number M of OCSS to be detected, their length L and the data width DW at the input can be modified according to the requirements of the application. Also, the final application of the proposed correlator in an U-LPS has been considered, and the number N_{SM} of carrier periods used in the modulation and the oversampling rate O_f can be also changed through synthesizing the design.

Note that, at every stage, the number of bits to store the partial correlation results is incremented. Thus, a reduction of the total memory required in the correlation is obtained when the larger delays D_n are placed at the first stage, and the smaller ones at the last stages. The delays have been implemented in specific shift registers in Xilinx FPGA's architectures (SRL16 primitives). Also, pipeline registers have been placed between substages to shorten the depth of combinational logic. Finally, it is important to emphasize that the multiplication operations by coefficients $\{w_{p,n}; 1 \leq p \leq log_2(M); 1 \leq n \leq N\}$ have been reduced to additions and subtractions. In fact these coefficients determine the final configuration of the adders and subtractors at every stage.

The design has been implemented in a Xilinx Virtex II XC2V8000 FPGA. Table IV shows the resource requirements and maximum throughput for different values of M and code lengths L when the number of bits of the input signal is $DW = 8$. This results can be compared with previous architectures, obtaining similar conclusions than those from Tables I to III. For instance, the optimized ESSC^T in [21] achieves 869 slices, 1455 LUTS and a maximum throughput of 112.18 Msamples/s when correlating the input signal with $M = 4$ OCSS of length $L = 64$. The M-times replication of the ESSC^T in [14], as well as the hardware implementation for interleaved complementary sequences proposed in [19], requires approximately M times more resources than the correlator implementation proposed here.

V. ARCHITECTURE OF THE LPS AND USE OF THE PROPOSED CORRELATOR

Fig. 5 shows a global view of the U-LPS used to test the proposed correlator. It consists of a set of four beacons placed at known positions in the ceiling of the environment, with a height of 3.50 m and inside a 0.67 $m \times 0.75$ m shape. These are the only devices to be installed. The beacons are hardware synchronized and they cover an area on the floor of 4.5 $m \times 4.5$ m. To avoid the MAI, the ultrasonic signals

TABLE III
EXAMPLE OF NUMBER OF OPERATIONS AND MEMORY BITS FOR THE SIMULTANEOUS CORRELATION OF M OCSS OF DIFFERENT LENGTHS L, WHEN THE DATA-WIDTH AT THE INPUT IS $DW = 8$

Architecture	$M = 4$, $L = 64$			$M = 8$, $L = 64$			$M = 16$, $L = 16$		
	Adders	Products	Memory	Adders	Products	Memory	Adders	Products	Memory
Straightforward	1020	1024	3072	4088	4096	8192	4080	4096	6144
M times replication of the ESSC^T [14]	108	48	5328	440	192	22 848	1264	512	23 040
Optimized ESSC^T [21]	60	24	1584	272	108	5600	1264	512	23 040
Proposed correlator	32	8	1332	72	12	2856	128	0	1440

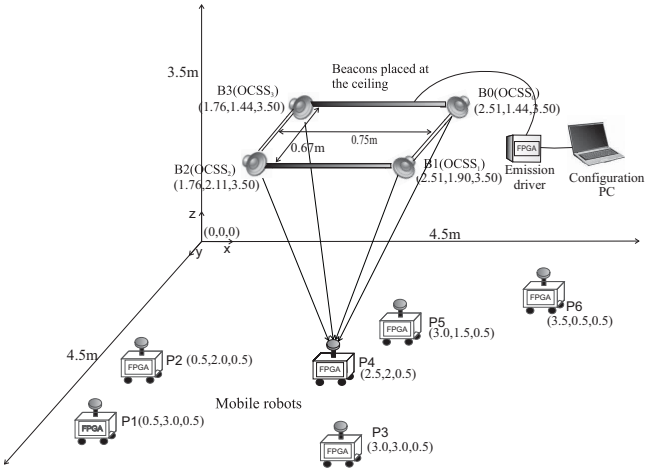

Fig. 5. Schematic representation of the U-LPS.

emitted by the beacons are encoded according to OCSS. Thus, each beacon periodically emits a different complementary set, orthogonal to those assigned to the other beacons. As will be explained in Section VI, the sequences of the set assigned to every beacon are transmitted in different time slots by using a BPSK modulation scheme. Inside the scanned area, mobile robots can detect the different transmissions and compute their local positions by hyperbolic trilateration. Fig. 5 also shows a set of test positions ($P1$ to $P6$) that have been used in Section VI to obtain some experimental results.

As can be observed in Fig. 6, the emission stage consists of three main modules: a configuration PC, an FPGA-based computing platform for emission driving, and the transducers. The configuration PC allows the real-time configuration of the ultrasonic emissions. The main parameters to be adjusted are the number L of bits of the OCSS, the type of carrier used in the modulation (square or sinusoidal), the number N_{SM} of carrier periods, the carrier frequency f_e and the time interval T_R between emissions. To obtain these parameters, the signal-to-noise ratio (SNR) supported by the system, the spectral features of the ultrasonic transducer and the length of the emission interval should be considered. The information regarding the OCSS to be emitted and the modulation symbol is generated off-line and stored in the PC. After the parameters of the ultrasonic emissions are determined, they are sent, together with the specific codes and modulation symbol, to the FPGA through an USB link.

The beacon emission driver has been designed in a Digilent Nexys-2 computing platform, which includes a Xilinx Spartan 3E-1200 FPGA, D/A converters and a USB port for communications with a PC. The codes and modulation symbol coming from the PC are stored in dual-port RAM memories in the FPGA. In each memory, one port is used by the USB interface to write the codes or the carrier, whereas the other port is used by the BPSK modulator. Every T_R the four memories with the codes are simultaneously read at the speed specified by the carrier frequency f_e. For each code bit the BPSK modulator directly transmits the carrier symbol (bit code=‘1’) or the reversed version of the carrier symbol (bit code=‘0’). The modulated codes are converted to analog and emitted by a set of four omni-directional piezoelectric polymer transducers by MSI [22], which have a resonant frequency of 40 kHz and a 8 kHz bandwidth.

TABLE IV
XC2V8000 UTILIZATION AND MAXIMUM THROUGHPUT FOR THE CORRELATION WITH THE PROPOSED ARCHITECTURE OF M OCSS OF LENGTH L

xc2v8000	$M = 4$, $L = 64$	$M = 8$, $L = 64$	$M = 16$, $L = 16$
Slices	489	955	1118
LUTs	669	1380	1790
IOBs	103	206	387
Max. throughput (Msamples/s)	136.8	110.7	160.8

The reception stage can be divided into three modules: an acquisition system, a low-level processing block and a high-level processing block. The acquisition system includes a Panasonic omni-directional electret microphone WM-61 [23], which has a flat frequency response between from 20 Hz to 45 kHz, and is oriented upward and placed on the top part of every mobile robot. In each robot, the signal acquired by the microphone is adapted by means of a preamplifier and an automatic control gain (SSM2166 preamplifier) to the input range of the Analog to Digital Converter (ADC). Then, the low-level processing module performs the digital demodulation, correlation and peak detection. These tasks have been implemented in a Xilinx Virtex II XC2V8000 FPGA, allowing the pre-synthesis configuration of the receiver parameters: sampling frequency f_s, data width DW, number of carrier periods N_{SM}, and size of correlators (the size of the correlators depends on the code length L). Obviously, these parameters have to be selected in concordance with those from the emission stage.

A digital squared carrier symbol has been used in the demodulation, thus, the BPSK demodulator has been imple-

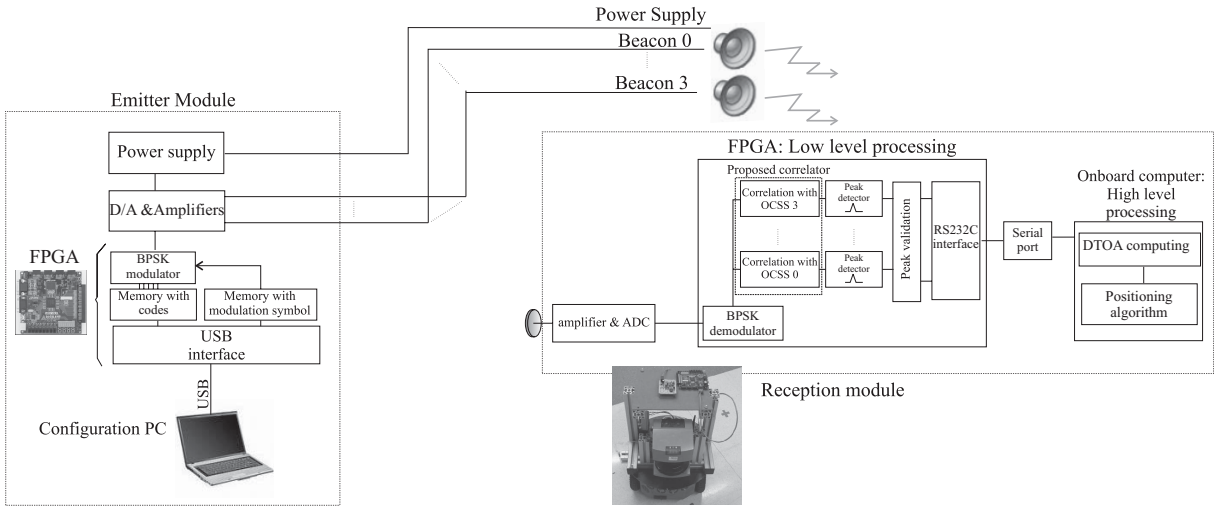

Fig. 6. Block Diagram of the proposed U-LPS.

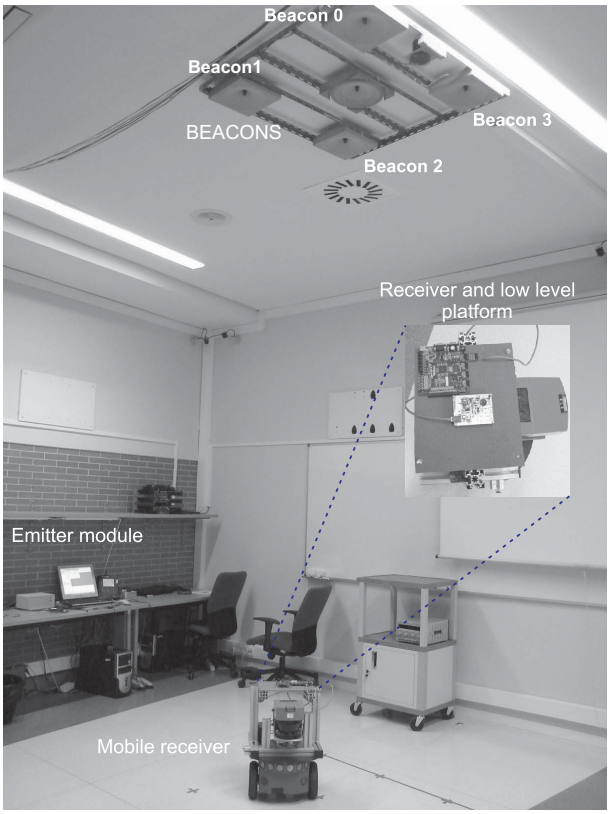

Fig. 7. Experimental set-up.

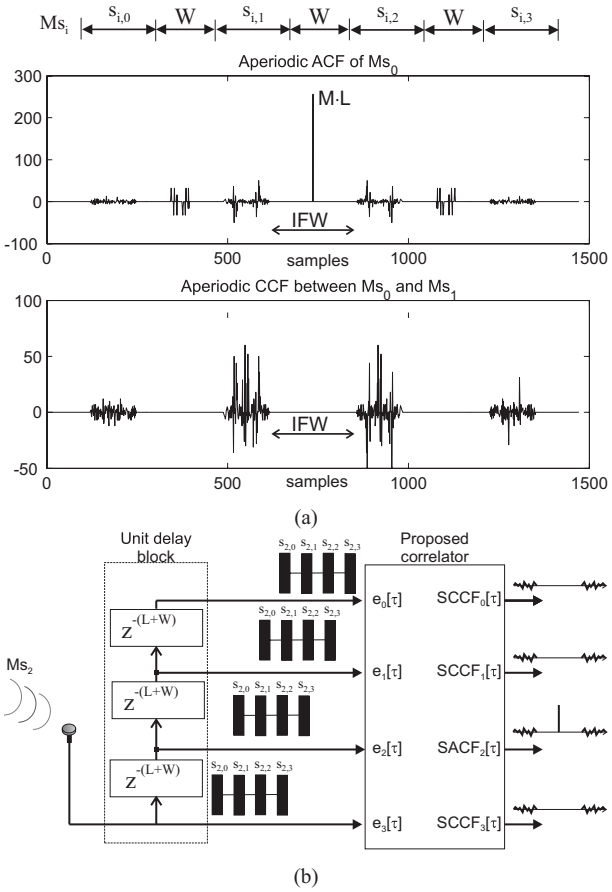

Fig. 8. (a) ACF and CCF of a macro-sequence $Ms_i(z) = \sum_{j=0}^{M-1} s_{i,j}\, z^{-j\cdot(L+W)}$. (b) Block diagram for the detection of a macro-sequence Ms_i.

mented as a shift register whose samples are added or subtracted. Afterwards, the demodulated signal is correlated with the corresponding code that identifies every beacon. These correlations have been carried out by using the algorithm described in Sections III and IV. When the last sample of a received code is processed, a local maximum is obtained only in the correlator matched to this code. A peak detector system at the output of each correlator searches for the local maxima that exceed a certain threshold, also configurable. The positions of the local maxima are sent through a serial RS232 port to the PC embedded in the robot, which is a PIONEER 3-DX8. The DTOAs are computed by assuming that the beacon $B0$ is the reference beacon and the sound speed is 345 m/s (temperature $T = 20$°C and humidity $H = 50\%$). Then, a hyperbolic trilateration based on the Caley-Menger bideterminant algorithm [24] uses the computed DTOAs to obtain the position of the mobile receiver.

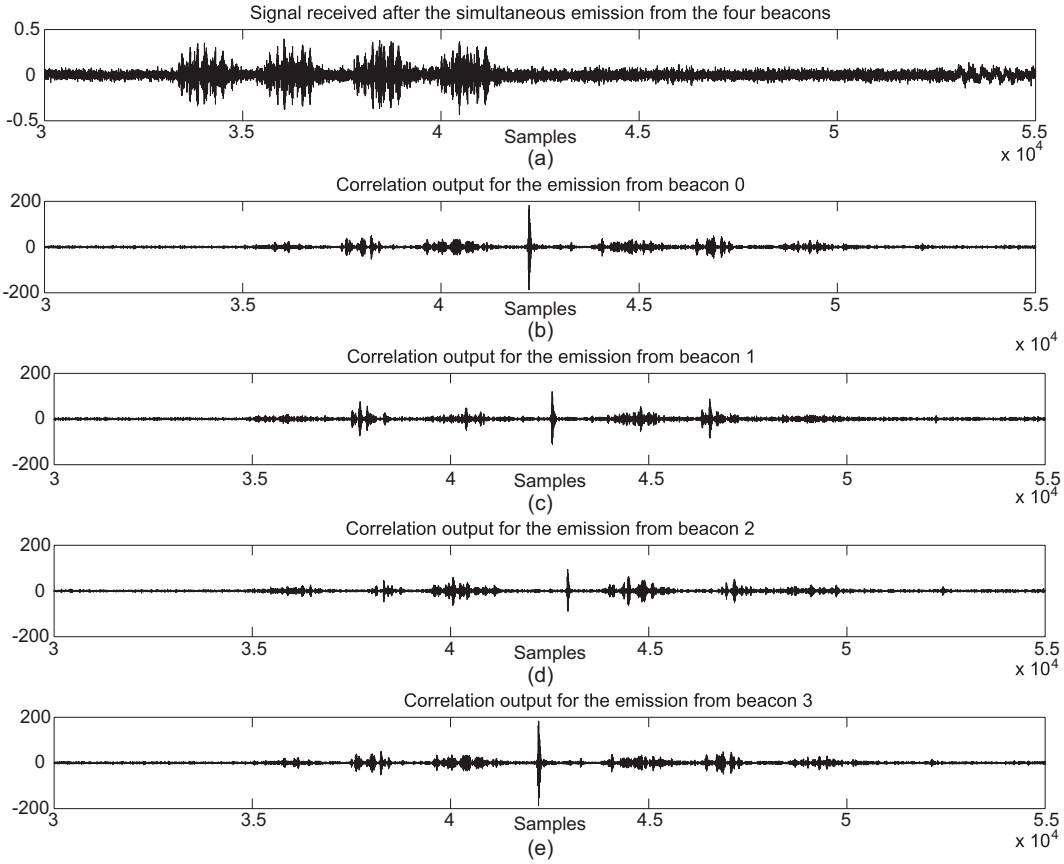

Fig. 9. (a) Received signal after the simultaneous emission from the four beacons. (b) Correlation outputs with the emissions corresponding to beacons 0, (c) 1, (d) 2, and (e) 3.

VI. Results

The architecture proposed in Section III has been applied to detect the arrival instant for each emission in a real U-LPS (see Fig. 7; note that the beacon in the middle is not used). The four beacons emit simultaneously every $T_R = 60\ ms$, each one a different OCSS with $M = 4$ sequences of length $L = 64$. To transmit the four sequences of the set S_i assigned to a beacon Bi, they have been concatenated in natural order and with a set of W zeros among them. Thus, a new macro-sequence $Ms_i(z) = \sum_{j=0}^{M-1} s_{i,j} z^{-j\cdot(L+W)}$ of length $L_{Ms} = M \cdot L + (M-1) \cdot W$ is obtained, and then transmitted by using a BPSK modulation. After this arranging method, the sum of correlation functions is no longer ideal. Nevertheless, the set of W zeros ensures an interference free window (IFW) around the in-phase shift (see Fig. 8.(a)). Taking into account the beacons location, the maximum distance among them and the size of the area to be covered, the maximum relative temporary offset between the codes is 2.2 ms (at 20°C) not to exceed this IFW. Thus, the W should be higher than 100. For more protection, the IFW has been fixed at $W = 120$ bits, what implies a macro-sequence length of 616 bits. Considering the frequency response of the transducer, the macro-sequences have been BPSK modulated with a $f_e = 41.67\ kHz$ sine carrier. Only one cycle $N_{SM} = 1$ per bit code has been used, in order not to increase the duration of the emissions.

In the reception, the acquisition system converts the signal received by the ultrasonic transducer with a $DW = 8$ bits data width. The sampling frequency is $f_s = 500\ kHz$, what provides an oversampling factor $O_f = 12$. With this sampling frequency, that exceeds the Nyquist requirements, a resolution of 2 μs in the determination of DTOAs can be reached, without the need of any interpolation technique (that permits a sub-centimeter precision in the position estimation). Note that the precision of the time of arrival measurement is bounded by the Cramer-Rao limit. In an active system, the achievable standard deviation σ of the time of flight determination can be obtained by (5) [26]:

$$\sigma^2 = \left(\frac{1}{8 \cdot \pi^2} \cdot \frac{1}{SNR} \cdot \frac{1}{T_o \cdot B} \cdot \frac{1}{f_e^2} \cdot \frac{1}{\left(1 + \frac{B^2}{12 \cdot f_e^2}\right)} \right) \quad (5)$$

where SNR is the signal-to-noise ratio; T_o is the signal duration in time ($T_o = \frac{L_{Ms}}{f_e}$ in this case); B is the bandwidth of the signal; and f_e is the central frequency of the emission. For the values considered in this case, with a transducer with a bandwidth of 8 kHz, the value σ is in the range of 0.25 μs, for a SNR as low as 0 dB.

After the acquisition, the received signal is demodulated and, considering the transmission scheme with macro-sequences, a unit delay block has to be included to obtain the in-phase addition of the correlation functions at the output (see Fig. 8.(b) for the detection of the macro-sequence Ms_2). This unit undoes the arranging performed in the construction of the macro-sequence: the correlator input associated to $s_{i,0}$ is

TABLE V
AVERAGE AND STANDARD DEVIATION OF DTDV WHEN THE FOUR BEACONS ARE SIMULTANEOUSLY EMITTING

Test point	Mean			Standard deviation		
	$DTOA_{1,0}$	$DTOA_{2,0}$	$DTOA_{3,0}$	$DTOA_{1,0}$	$DTOA_{2,0}$	$DTOA_{3,0}$
P1 (0.5,3.0,0.5)	–59.35 μs	–1600.00 μs	–927.47 μs	11.36 μs	11.86 μs	11.33 μs
P2 (0.5,2.0,0.5)	–113.35 μs	–1100.00 μs	–997.62 μs	11.34 μs	11.43 μs	11.40 μs
P3 (3.0,3.0,0.5)	–671.14 μs	–133.51 μs	527.08 μs	9.37 μs	9.22 μs	9.57 μs
P4 (2.5,2.0,0.5)	123.94 μs	120.56 μs	261.83 μs	0.89 μs	0.91 μs	1.20 μs
P5 (3.0,1.5,0.5)	182.76 μs	740.47 μs	587.35 μs	11.31 μs	0.86 μs	0.94 μs
P6 (3.5,0.5,0.5)	674.26 μs	1500.00 μs	829.03 μs	1.81 μs	0.78 μs	1.01 μs

delayed $z^{-552\cdot 12}$ samples, the one associated to $s_{i,1}$ is delayed $z^{-368\cdot 12}$ samples, the associated to $s_{i,2}$ is delayed $z^{-184\cdot 12}$ samples and, finally, the one associated to $s_{i,3}$ (which is the last complementary sequence to be received) is not delayed. Thus, there is a temporary interval where the different sequences of the set S_i are simultaneously processed in the proposed correlator. During that interval the SACF and SCCF at the output show ideal properties.

To check the feasibility of the OCSS-based U-LPS, six test points have been considered in different positions in the environment (see $P1$ to $P6$ in Fig. 5). A set of 100 consecutive measurements has been made at each position. Fig. 9.(a) shows the signal received after one emission at the test point $P6$. The four emitted macro-sequences Ms_0 to Ms_3 are received altogether, and the gap W between sequences $s_{i,j}$; $0 \leq j \leq M-1$ can be observed. Figs 9.(b), (c), (d) and (e) depict the correlation outputs for beacons $B0$, $B1$, $B2$ and $B3$ respectively. The IFW around the auto-correlation peak can be observed in all of them. Since the relative multiple access delays are within this IFW, the ISI and MAI interferences are significantly reduced. Therefore, the code emitted by beacon $B0$, which is the closest to the test point $P6$, does not mask the weak signal coming from beacon $B2$, located further away.

Table V details the average and standard deviation of the DTOAs assuming that beacon $B0$ is the reference. Hence, $DTOA_{i,0}$ is the difference between the arrival time corresponding to the emission from beacon Bi and beacon $B0$. As can be observed, the variations in the DTOAs are below 6 samples (12 μs) in all cases. Note that the error is lower than half a bit code duration, what means that the positioning can be achieved with subcentimeter-accuracy.

Similar tests have been done in [16] to compare the performance of different codes derived from OCSS in an ULPS. The maximum length L of that codes and number M of simultaneous emissions are constrained by the correlator implementation. By using the architecture proposed here real-time detection of very long OCSS is possible.

VII. CONCLUSION

A new architecture for the correlation of orthogonal complementary sets of sequences (OCSS) has been presented. This architecture outperforms previous solutions found in literature in terms of operation number and memory requirements. It constitutes the kernel of the detection stage of an Ultrasonic Local Positioning System (U-LPS), which has been also presented. To achieve multi-emission, the signals emitted from the beacons of the U-LPS have been encoded with OCSS. Then, by using the proposed architecture, portable receivers simultaneously compute the correlation with all the emitted codes, thus obtaining the maximum peaks that determine the arrival instant of each emitted OCSS. The absolute position is determined by hyperbolic trilateration, using the Differences in Times Of Arrival (DTOA) between a reference beacon and the others.

Real test have been done to verify that the proposed correlator simplifies the hardware implementation and allows the real-time processing of the ultrasonic signals coming from the beacons, which have been encoded with $M = 4$ OCSS with sequence-length $L = 64$. The results show a significant reduction in the sidelobe effects of the correlation outputs within a region around the zero shift. The standard deviations of the DTOAs are below 12 μs, what means a subcentimeter precision in the position estimation.

REFERENCES

[1] J. C. Prieto, A. R. Jiménez, J. Guevara, J. Ealo, F. Seco, J. Roa, and A. Koutsou, "Performance evaluation of 3D–LOCUS advanced acoustic LPS," *IEEE Trans. Instrum. Meas.*, vol. 58, no. 8, pp. 2385–2395, Aug. 2009.

[2] E. A. Prigge and J. P. How, "Signal architecture for a distributed magnetic local positioning system," *IEEE Sensors J.*, vol. 4, no. 6, pp. 864–873, Dec. 2004.

[3] M. Hazas and A. Hooper, "Broadband ultrasonic location system for improved indoor positioning," *IEEE Trans. Mobile Comput.*, vol. 5, no. 8, pp. 536–547, May 2006.

[4] Y. Lu and A. Finger, "Ultrasonic beacon-based local position system using broadband PN (pseudo-noise)-chirp codes," in *Proc. 9th IASTED Int. Conf. Wireless Opt. Commun.*, Aug. 2009, pp. 1–6.

[5] J. M. Villadangos, J. Ureña, J. J. García, M. Mazo, A. Hernández, A. Jiménez, D. Ruíz, and C. De Marziani, "Measuring time-of-flight in an ultrasonic LPS system using generalized cross-correlation," *Sensors*, vol. 11, no. 11, pp. 10326–10342, 2011.

[6] S. Wang and A. Abdi, "MIMO ISI channel estimation using uncorrelated golay complementary sets of polyphase sequences," *IEEE Trans. Veh. Technol.*, vol. 56, no. 5, pp. 3024–3039, Sep. 2007.

[7] A. Nowicki, I. Trots, P. A. Lewin, W. Secomski, and R. Tymkiewicz, "Influence of the ultrasound transducer bandwidth on selection of the complementary Golay bit code length," *Ultrasonics*, vol. 47, nos. 1–4, pp. 64–73, 2007.

[8] P. Smith, C. Furse, and J. Gunther, "Analysis of spread spectrum time domain reflectometry for wire fault location," *IEEE Sensors J.*, vol. 5, no. 6, pp. 1469–1478, Dec. 2005.

[9] N. Levanon, "Noncoherent radar pulse compression based on complementary sequences," *IEEE Trans. Aerosp. Electron. Syst.*, vol. 45, no. 2, pp. 742–747, Apr. 2009.

[10] C. Zhang, S. Yamada, and M. Hatori, "General method to construct LS codes by complete complementary sequences," *IEICE Trans. Wireless Commun. Technol.*, vol. E88-B, no. 8, pp. 3484–3487, Aug. 2005.

[11] H. Cheng, C. Wu, C. Yang, and Y. Chang, "Wavelength division multiplexing/spectral amplitude coding in applications in fiber vibration sensor systems," *IEEE Sensors J.*, vol. 11, no. 10, pp. 2518–2526, Oct. 2011.
[12] J. Li, A. Huang, M. Guizani, and H. Chen, "Inter-group complementary codes for interference-resistant CDMA wireless communications," *IEEE Trans. Wireless Commun.*, vol. 7, no. 1, pp. 166–174, Jan. 2008.
[13] M. A. Funes, P. G. Donato, M. N. Hadad, and D. O. Carrica, "Reduced architecture for simultaneous correlation of orthogonal sets of complementary sequences," *Electron. Lett.*, vol. 46, no. 22, pp. 1502–1504, 2010.
[14] C. De Marziani, J. Ureña, A. Hernández, J. J. García, F. Álvarez, A. Jiménez, and M. C. Pérez, "Recursive algorithm to directly obtain the sum of correlations in a CSS," *Signal Process.*, vol. 91, no. 5, pp. 1343–1346, 2011.
[15] F. J. Álvarez, A. Hernández, J. Ureña, M. Mazo, J. J. García, J. A. Jiménez, and A. Jiménez, "Real-time implementation of an efficient correlator for complementary sets of four sequences applied to ultrasonic pulse compression systems," *Microprocess. Microsyst.*, vol. 30, no. 1, pp. 43–51, 2006.
[16] M. C. Pérez, J. Ureña, A. Hernández, A. Jiménez, F. J. Álvarez, and C. De Marziani, "Performance comparison of different codes in an ultrasonic positioning sytem using DS-CDMA," in *Proc. 6th IEEE Int. Symp. Intell. Signal Process.*, Aug. 2009, pp. 125–130.
[17] S. Z. Budisin, "Efficient pulse compressor for golay complementary sequences," *Electron. Lett.*, vol. 27, no. 3, pp. 219–220, Jan. 1991.
[18] C. Marziani, J. Ureña, A. Hernández, M. Mazo, F. Álvarez, J. García, and P. Donato, "Modular architecture for efficient generation and correlation of complementary sets of sequences," *IEEE Trans. Signal Process.*, vol. 55, no. 5, pp. 2323–2337, May 2007.
[19] M. C. Pérez, J. Ureña, A. Hernández, C. De Marziani, and A. Jiménez, "Hardware implementation of an efficient correlator for interleaved complementary sets of sequences," *J. Universal Comput. Sci.*, vol. 13, no. 3, pp. 388–406, Mar. 2007.
[20] P. G. Donato, M. A. Funes, M. N. Hadad, and D. O. Carrica, "Simultaneous correlation of orthogonal pairs of complementary sequences," *Electron. Lett.*, vol. 45, no. 25, pp. 1332–1334, 2009.
[21] M. C. Pérez, J. Ureña, A. Hernández, C. De Marziani, J. J. García, and A. Jiménez, "Optimized correlator for LS codes-based CDMA systems," *IEEE Commun. Lett.*, vol. 15, no. 2, pp. 223–225, Feb. 2010.
[22] Measurement Specialties, Inc. (2012). *40 kHz Omni-Directional Ultrasound Transmitter*, Hampton, VA [Online]. Available: http://www.meas-spec.com
[23] Panasonic Industrial Components. (2012). *Audio Electret Condenser Microphone. Omnidirectional Back Electret Condenser Microphone Cartridge*, Secaucus, NJ [Online]. Available: http://www.panasonic.com
[24] D. Ruiz, J. Ureña, I. Gude, J. M. Villadangos, J. C. García, M. C. Pérez, and E. García, "Hyperbolic ultrasonic LPS using a Caley-Menger bideterminant-based algorithm," in *Proc. IEEE Instrum. Meas. Technol. Conf.*, May 2009, pp. 785–790.
[25] A. Oppenhein, R. Shafer, and J. Buck, *Discrete-Time Signal Processing*, 2nd ed. Englewood Cliffs, NJ: Prentice-Hall, 1999.
[26] A. H. Quazi, "An overview of the time delay estimate in active and passive systems for target localization," *IEEE Trans. Acoust. Speech, Signal Process.*, vol. 29, no. 3, pp. 527–533, Jun. 1981.

M. Carmen Peréz Rubio (M'07) received the M.S. degree in electronics engineering and the Ph.D. degree from the University of Alcalá, Madrid, Spain, in 2004 and 2009, respectively.

She is currently an Assistant Professor with the Electronics Department, University of Alcalá. Since 2003, she has been engaged in several research projects in the areas of sequence design, low-level ultrasonic signal processing, and computing architectures.

Rebeca Sanz Serrano received the M.S. degree in telecommunications engineering and the M.S. degree in advanced electronic systems from the University of Alcalá, Madrid, Spain, in 2010 and 2011, respectively.

She is currently a Design Engineer for embedded systems in a Video Broadcast Company. She has been engaged in several projects in the areas of CDMA sequence design, local positioning systems, and mobile robotics, since 2008.

Jesús Ureña Ureña (M'06) received the B.S. degree in electronics engineering and the M.S. degree in telecommunications engineering from the Polytechnical University of Madrid, Madrid, Spain, in 1986 and 1992, respectively, and the Ph.D. degree in telecommunications from the University of Alcalá, Madrid, in 1998.

He has been with the Department of Electronics, University of Alcalá, as a Professor, since 1986. From 1993 to 1997, he was the Head of the Department. He has engaged in several educational and research projects in the area of electronic control and sensorial systems for mobile robots and wheelchairs, and in the area of electronic-distributed systems for railways. His current research interests include low-level ultrasonic signal processing, local positioning systems, and sensory systems for railway infrastructure.

Álvaro Hernańdez Alonso (M'06) received the Ph.D. degree from the University of Alcalá, Madrid, Spain, and Blaise Pascal University, Clermont-Ferrand, France, in 2003.

He is currently an Associate Professor of Digital Systems and Electronic Design with the Electronics Department, University of Alcalá. His current research interests include multisensor integration, electronic systems for mobile robots, and digital and embedded systems.

Carlos De Marziani received the Electronics Engineering degree from the University of Patagonia San Juan Bosco, Comodoro Rivadavia, Argentina, in 2001, and the Ph.D. degree from Electronics Department, University of Alcalá, Madrid, Spain, in 2007.

He is currently a Professor of Digital Systems with the Electronics Department, University of Patagonia San Juan Bosco, and an Assistant Researcher with the National Council on Scientific and Technical Research, Consejo Nacional de Investigaciones Científicas y Técnicas, Argentina. His current research interests include sensor networks, multisensor integration, electronic systems for mobile robots, and digital signal processing.

Fernando J. Álvarez Franco (M'07) received the Degree in physics from the University of Seville, Seville, Spain, in 1998, and the Ph.D. degree in electronics from the University of Alcalá, Madrid, Spain, in 2006.

He is currently an Associate Professor of Digital Electronics with the Department of Electrical Engineering, Electronics and Automatics, University of Extremadura, Plasencia, Spain, where he is the Head of the Sensory Systems Group. His current research interests include local positioning systems, ultrasonic signal processing, and outdoor acoustics.